2.2 Calculated depositions

Four EMEP Centres Joint Reports for HELCOM (Tarrason *et al*. 1997; Bartnicki *et al*. 1998, 2000, 2001) have been published before the present one. Except the first report, all of them were focused on the annual results. Present report is more similar to the first one because all computations presented and discussed in it cover 5-year period: 1996 – 2000.

The calculations of nitrogen depositions presented in this report have been performed with a new version of the EMEP Eulerian model, the so-called Unified model (EMEP, 2002). The latest version of this model (revision rv1.2) enables explicit calculation of the stomatal and non-stomatal components of surface fluxes to each land-use class within a grid square. The deposition module has previously been examined and tested mainly for ozone (Emberson *et al*., 2000a, 2000b, 2001; Simpson *et al.*, 2001, Tuovinen *et al*., 2001), but has been extended to cope with the other EMEP gases. It should be noted that this new module gives rather different deposition rates for species such as NO_2 and NH_3 compared to earlier versions.

The calculation of sub-fluxes has in fact been included in the EMEP acidification models (Tsyro 1998, Olendrzynski 1999), albeit with much simpler treatments of vegetation and seasonal patterns. However, in previous versions the results of these sub-grid calculations were aggregated to grid-square averages before output of deposition estimates. In the new model version, no such aggregation is done, and deposition rates for each type of land use are explicitly exported from the model.

This new procedure has a number of implications for the estimates of N deposition to sea areas, at least for those grids containing both land and sea areas. Species such as NO_2, which are relatively insoluble will have little deposition to sea areas, but deposition over land can be significant. On the other hand, NH_3 is a relatively soluble gas and deposition to sea may be enhanced compared to land-areas.

For computation of airborne transport and depositions and source allocation budgets of cadmium, lead, and mercury within the EMEP domain Eulerian three-dimensional operational MSCE-HM model was used. The model vertical structure consists of five non-uniform layers and covers the entire planetary boundary layer and a part of the free troposphere. Horizontal resolution is 50x50 km. The model includes processes of advection, turbulent diffusion, wet and dry removal and chemical transformations of mercury. Deposition rates are calculated explicitly for each type of land use and water surface. A detailed description of the model can be found in EMEP reports (Ryaboshapko *et al.*, 1999; Ilyin *et al.*, 2001) on EMEP web page http://www.emep.int in the Internet under the link to information on Heavy Metals.

Modeling results for γ-HCH were obtained using the three-dimensional Eulerian multimedia POP transport model (MSCE-POP), which is being developed at MSC-E. The model is operating within the geographical scope of the EMEP region both with spatial resolution 50×50 km (135×111 cells) and 150x150 km (45x37 cells). It includes the following basic processes: advective transport, turbulent diffusion, dry and wet deposition, gas/particle partitioning, degradation, and gaseous exchange between the atmosphere and different types of underlying surface (soil, seawater, vegetation). The model considers the following compartments: air, soil, sea, vegetation and forest litter fall. The detailed description of MSCE-POP long-range transport model is given in several EMEP reports (Pekar *et al.*, 1999; Shatalov *et al.*, 2000; Shatalov *et al*., 2001) and on EMEP web page http://www.emep.int in the Internet under the link to information on Persistent Organic Pollutants.

2.1.1 Maps of annual depositions to the Baltic Sea

In this section we compare annual deposition maps for the year 1996 (beginning of the 5-year period) with annual deposition maps for the year 2000 (end of the five year period). Comparison includes all components.

Annual deposition maps (1996 vs 2000) for oxidized, reduced and total nitrogen are shown in Figures 2.15, 2.16 and 2.17, respectively. The same scale is used for all three figures. More deposition of reduced nitrogen can be noticed in 2000 than in 1996, especially in the South-West Baltic, but also to less extent in the Northern Baltic. The same remark applies to the deposition of total nitrogen.

Annual deposition maps for cadmium, lead, and mercury are presented in Figures 2.18, 2.19, and 2.20, respectively. Computed cadmium deposition fluxes over the Baltic Sea for 1996 and 2000 do not differ significantly (Figure 2.18). Some decrease can be noticed over the north-western part and south-eastern coast of Baltic Proper. Lower values of deposition fluxes in 2000 take place for the Gulf of Bothnia. At the same time cadmium deposition fluxes over the Belt Sea are higher in 2000 comparing to 1996. Similar to cadmium there is no significant changes in lead deposition fluxes over the Baltic Sea in the considered period (Figure 2.19). Slightly decreased lead deposition fluxes can be indicated over the north-western part of the Baltic Proper and over the Gulf of Bothnia in 2000. Mercury deposition fluxes over the Gulf of Bothnia, Gulf of Finland, and Gulf of Riga in 1996 are practically the same comparing to 2000. Over the southern part of the Baltic Proper, Belt Sea, and Kattegat an increase of mercury deposition fluxes in 2000 can be indicated (Figure 2.20). Modeling results for lindane (γ-HCH) cover only part of the considered 5-year period, in particular, 1996-1998. During these three years computed annual lindane (γ-HCH) net deposition fluxes to the Baltic Sea did not change significantly. Therefore, to characterize the level of lindane depositions to the Baltic Sea the spatial distribution of net depositions is given for 1998 (Figure 2.2X). The most significant values of lindane deposition fluxes can be indicated for south-western part of the Baltic Sea - Belt Sea and Kattegat sub-basins.

2.1.2 Time series of annual depositions to sub-basins

Here we present the time series of annual depositions to six main sub-basins of the Baltic Sea in the period 1996 – 2000 and for all components.

Time series for total, oxidized and reduced nitrogen are shown in Figures 2.21, 2.22 and 2.23, respectively. Concerning total nitrogen, increased deposition in 2000 compared to deposition in 1996 can be observed in four sub-basins: Gulf of Bothnia, Baltic Proper, Belt Sea and Kattegat. Larger 2000 annual deposition in four sub-basins is mainly caused by larger deposition of reduced nitrogen (Fig. 2.23) in the same sub-basins in 2000. Annual depositions of oxidized nitrogen (Fig. 2.22) do not change so much during the 5-year period.

All types of nitrogen depositions are scattered in the 5-year period, most likely due to variable meteorological conditions each year. No significant trend is visible in any type of annual nitrogen deposition.

Time series of cadmium, lead, mercury, and lindane annual depositions are presented in Figures 2.21, 2.22, 2.23, and 2.24, respectively. Similar to nitrogen compounds no significant trend can be indicated in computed depositions of heavy metals to the Baltic Sea sub-basins in 1996-2000. Changes in annual depositions of heavy metals to the Baltic Sea are most likely caused by variation of meteorological conditions in the 5-year period. Maximum deposition values in most of sub-basins of the Baltic Sea take place for cadmium in 1997, for lead in 1998, and for mercury in 2000. According to modelling results, atmospheric depositions of lead and cadmium to the Baltic Sea within the considered 5-year period have decreased by approximately 4%, whereas atmospheric depositions of mercury have increased by 14%.

Time-series of lindane (γ-HCH) depositions indicate substantial decrease of annual depositions to the Baltic Sea sub-basins during the period 1970-1998. In particular, most significant changes in depositions took place in 70s and 80s. During 1996-1998 annual depositions in Gulf of Bothnia, Gulf of Finland, and Gulf of Riga sub-basins do not change significantly. In south-western part of the Baltic Sea (Baltic Proper, Kattegat, and the Belt Sea sub-basins) some increase in lindane (γ-HCH) depositions within this period can be indicated. Level of annual volatilization of lindane from the Baltic Sea is generally lower for all sub-basins within the considered period.

2.1.3 Seasonal variability of computed depositions

Seasonal variation of computed monthly depositions to the Baltic Sea is presented in the form of five separate lines, one for each year of the 1996 – 2000 period.

In case of monthly depositions of total nitrogen, two local maxima are visible, one for June and one for October – November. The first one is stronger, because it occurs in four years out of 5-year period and the second occurs only in 2-3 years of the 5-year period.

Variations of computed lead, cadmium, and mercury depositions are presented in Figures 2.31, 2.32, and 2.33. As seen from figures seasonal changes of depositions of these heavy metals have similar character. Higher deposition values can be indicated for winter period. For mercury higher deposition values also take place in summer.

Seasonal pattern of lindane net depositions to the Baltic Sea for 1996-1998 is shown in Figure 2.34. Due to pronounced temporal variation of emissions and influence of meteorological conditions, monthly net deposition fluxes of lindane vary significantly during each year and also from year to year. It is assumed that maximum of emissions take place in spring time. Following this, maximum values of deposition fluxes are obtained for the spring months. During the second part of the year, when the emission in absent, the re-emission process prevails.

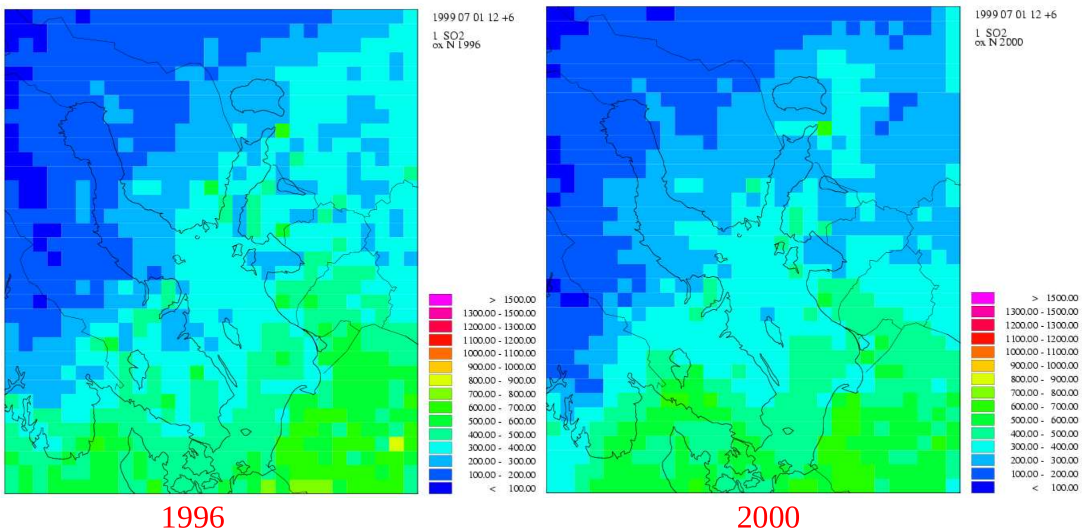

Figure 2.15. Maps of calculated, annual average depositions of oxidized nitrogen in the years 1996 and 2000. Units: mg N/m^2/yr.

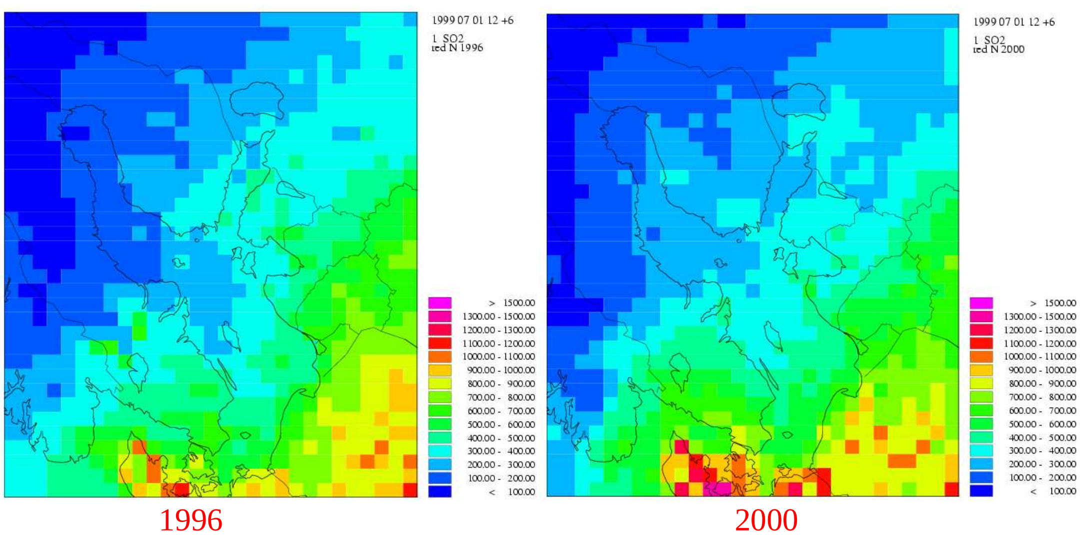

Figure 2.16. Maps of calculated, annual average depositions of reduced nitrogen in the years 1996 and 2000. Units: mg/m^2/yr.

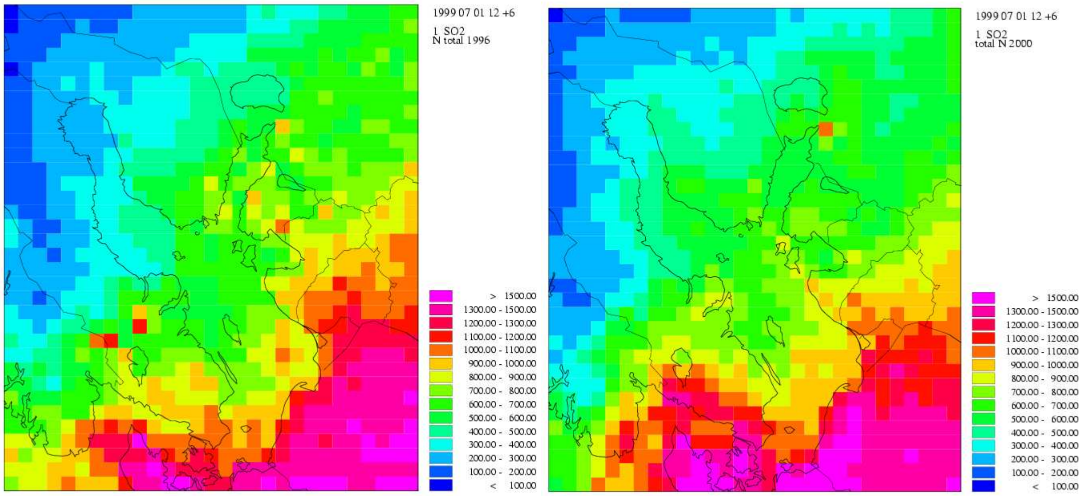

1996 2000

Figure 2.17. Maps of calculated, annual average depositions of total (oxidized plus reduced) nitrogen in the years 1996 and 2000. Units: mg/m^2/yr.

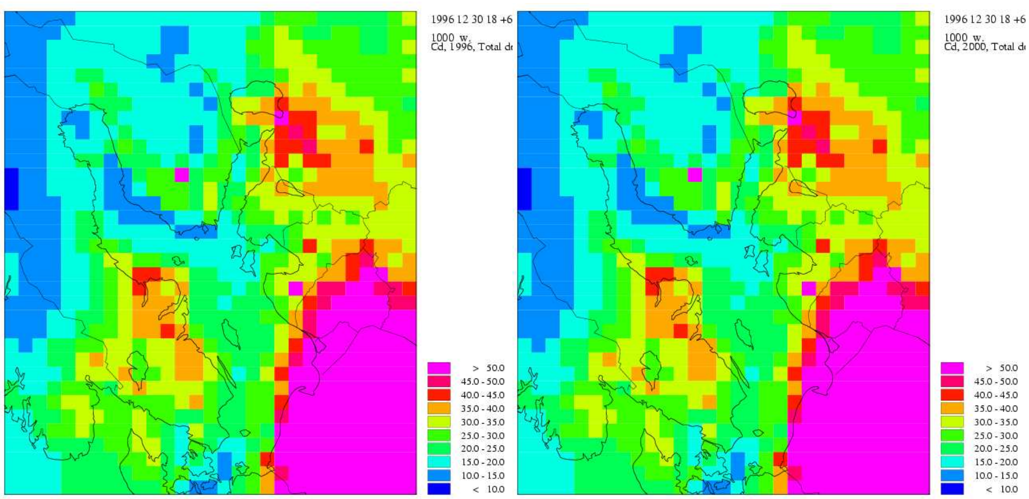

1996 2000

Figure 2.18. Maps of calculated, annual average depositions of cadmium in the years 1996 and 2000. Units: g/km^2/yr.

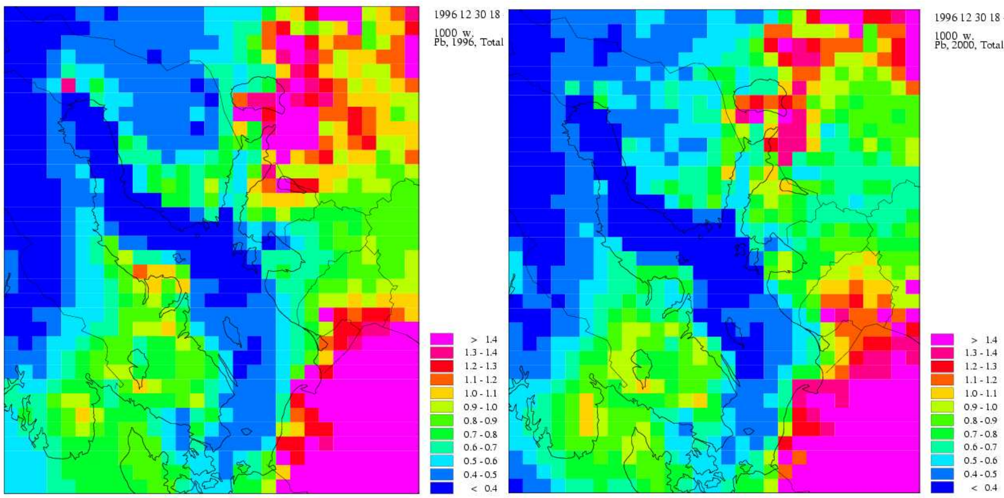

1996 2000

Figure 2.19. Maps of calculated, annual average depositions of lead in the years 1996 and 2000. Units: kg/km^2/yr.

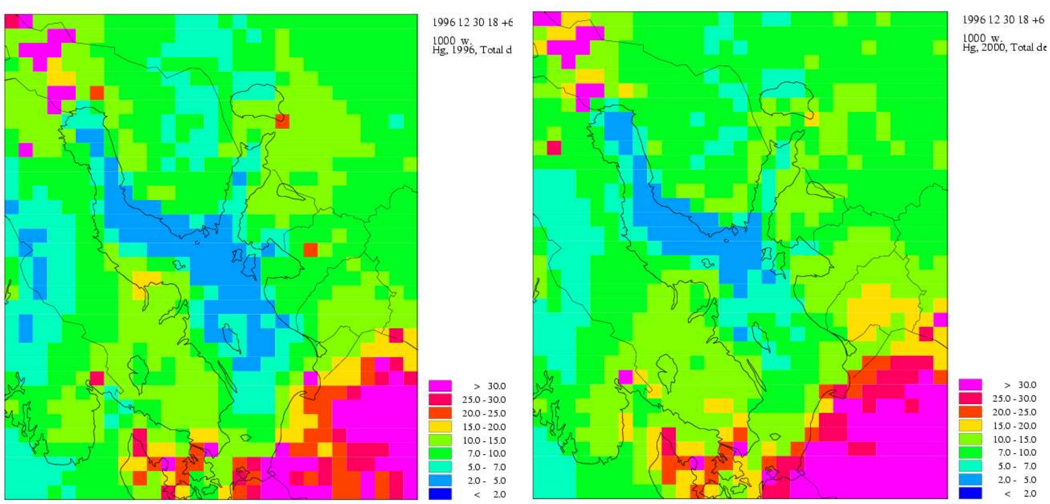

1996 2000

Figure 2.20. Maps of calculated, annual average depositions of mercury in the years 1996 and 2000. Units: g/km^2/yr.

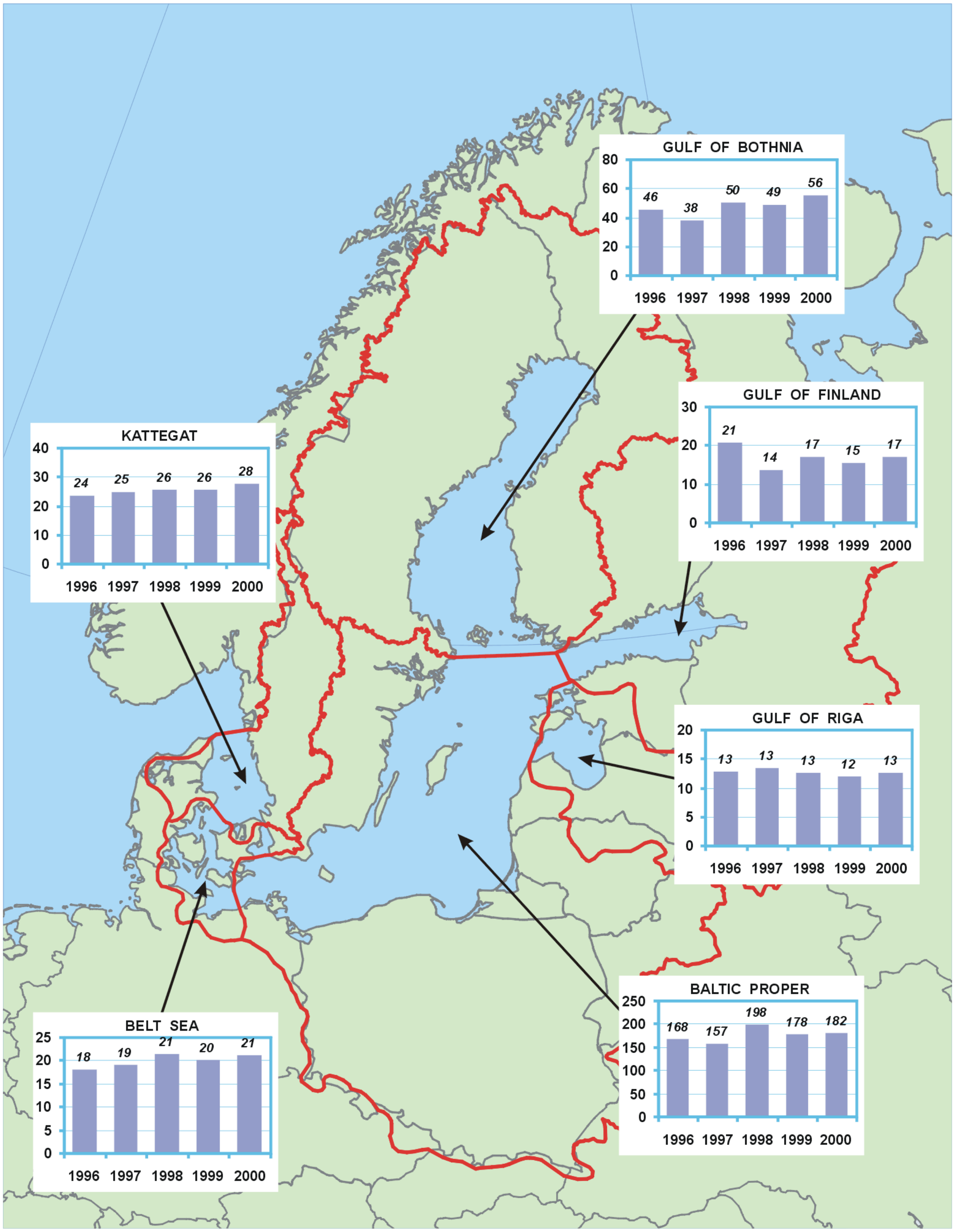

Figure 2.21. Time series of total nitrogen deposition to six main sub-basins of the Baltic Sea in the period 1996-2000. Units: ktones/yr.

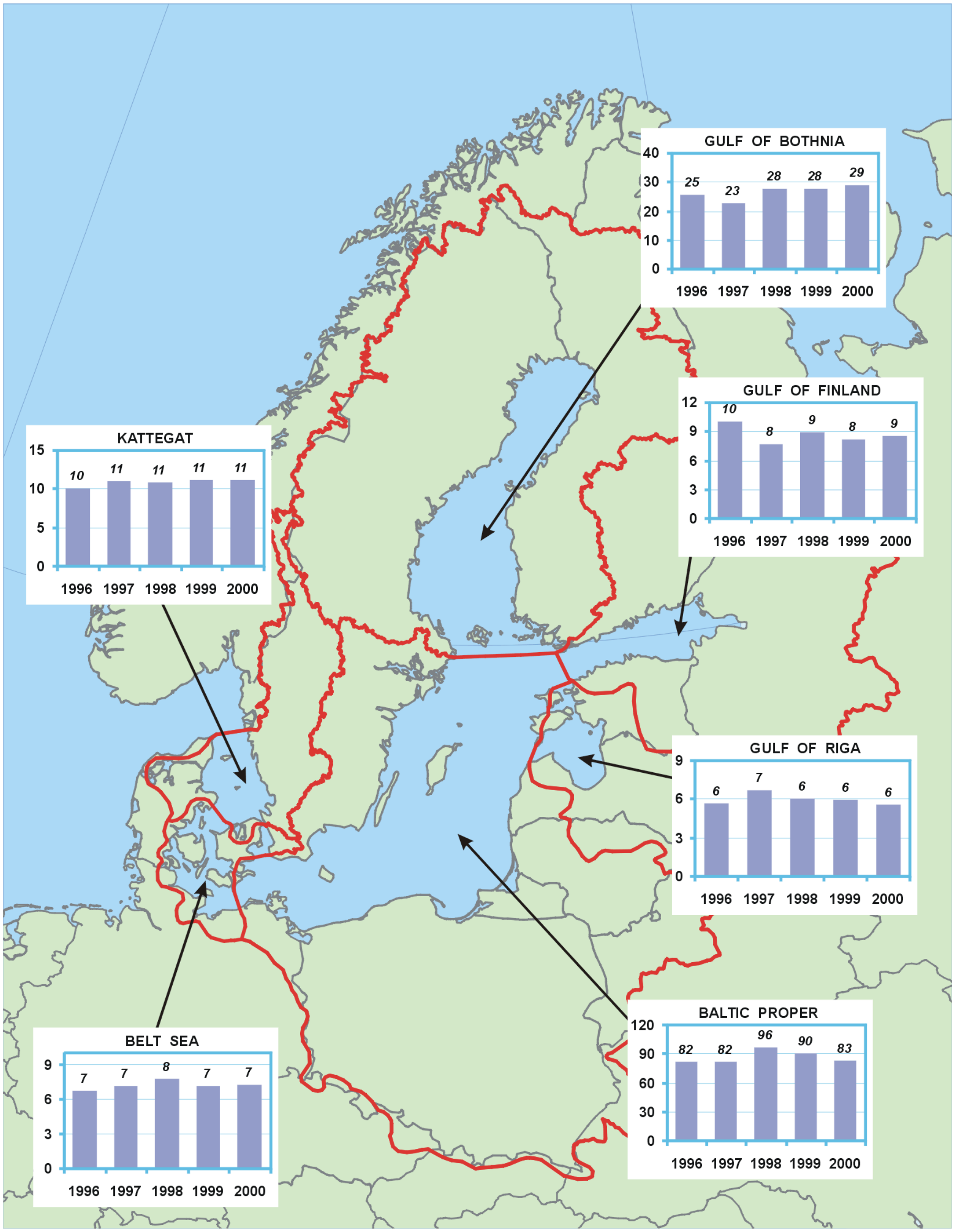

Figure 2.22. Time series of oxidized nitrogen deposition to six main sub-basins of the Baltic Sea in the period 1996-2000. Units: ktones/yr.

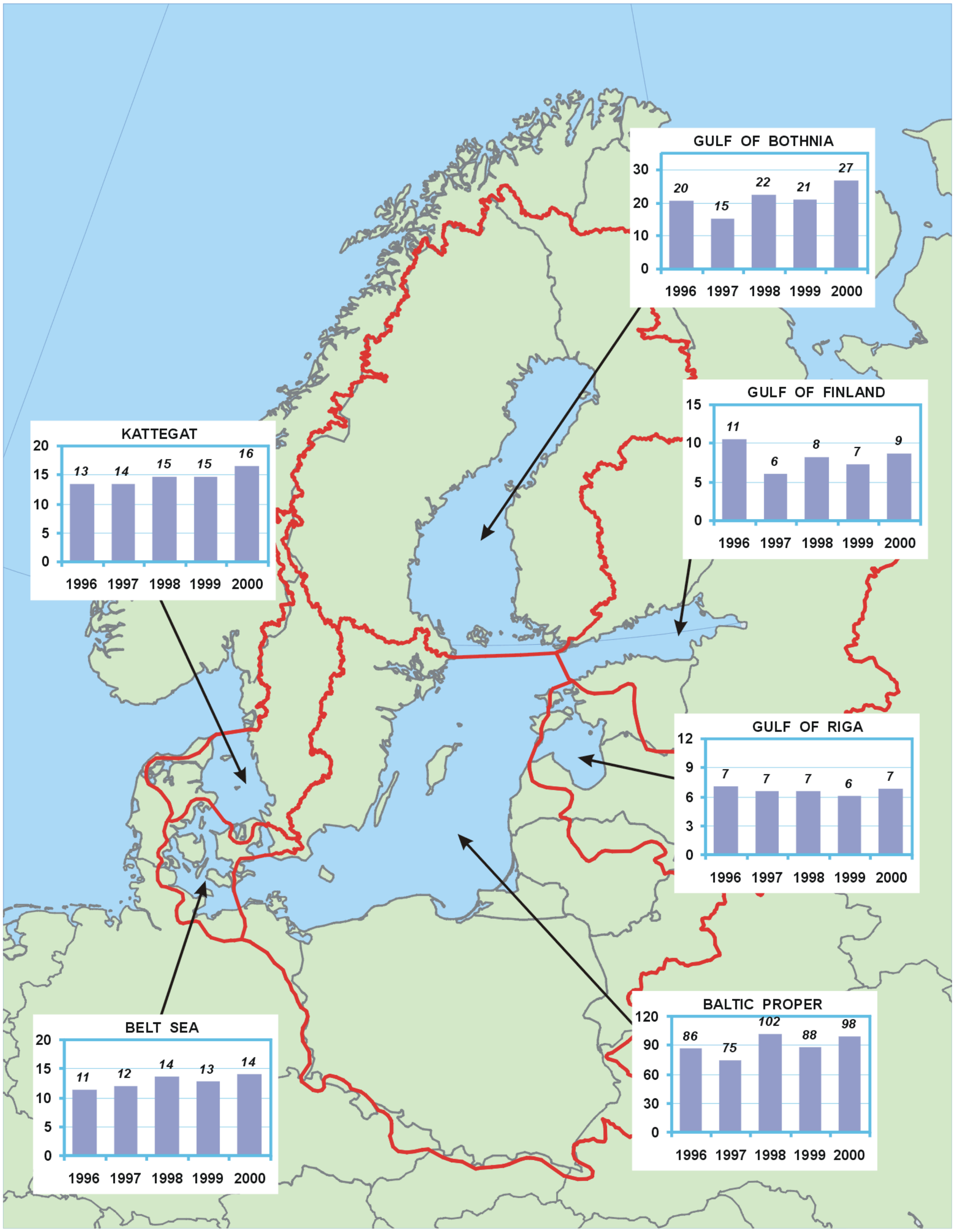

Figure 2.23. Time series of reduced nitrogen deposition to six main sub-basins of the Baltic Sea in the period 1996-2000. Units: ktonnes/yr.

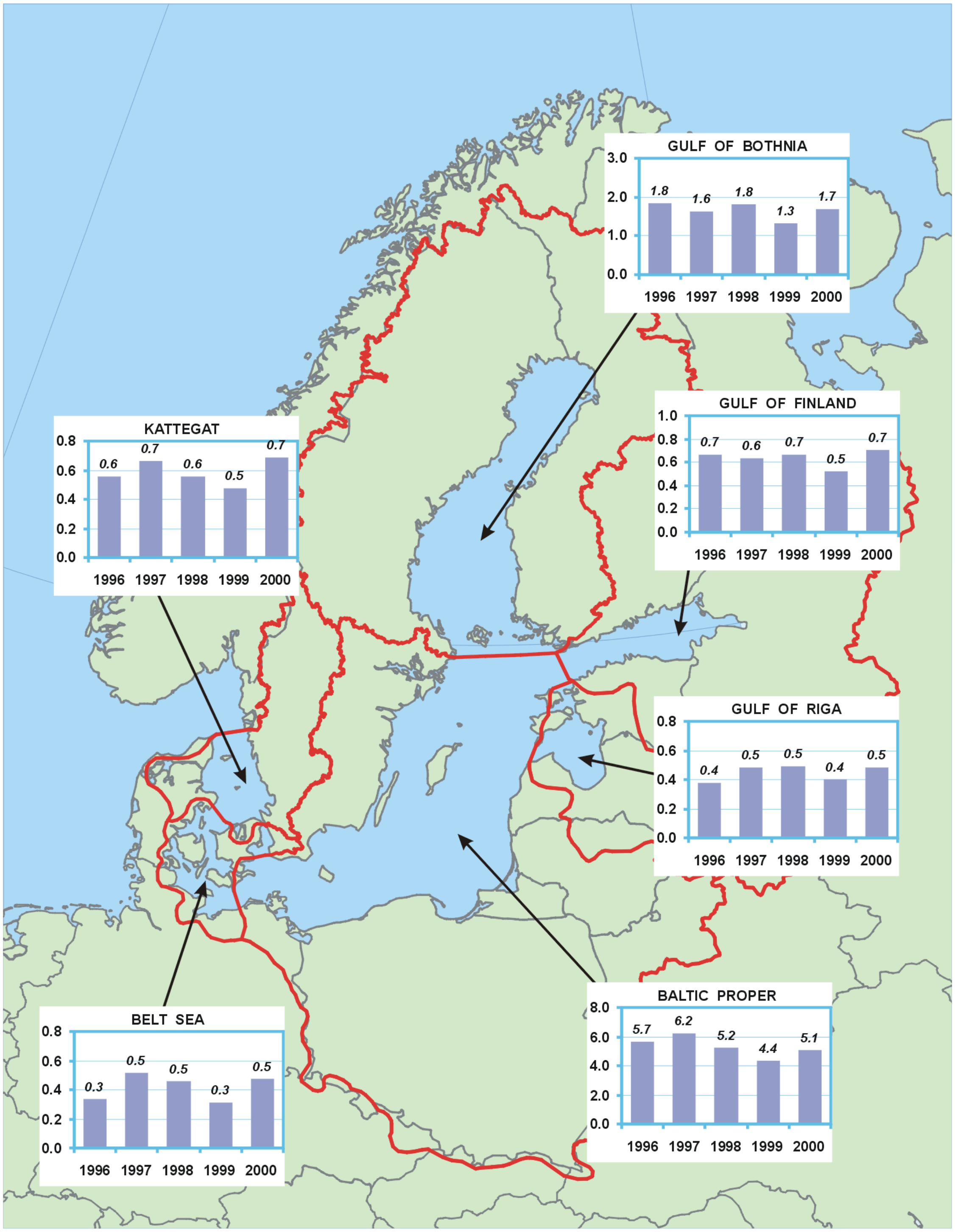

Figure 2.24. Time series of cadmium deposition to six main sub-basins of the Baltic Sea in the period 1996-2000. Units: tones/yr.

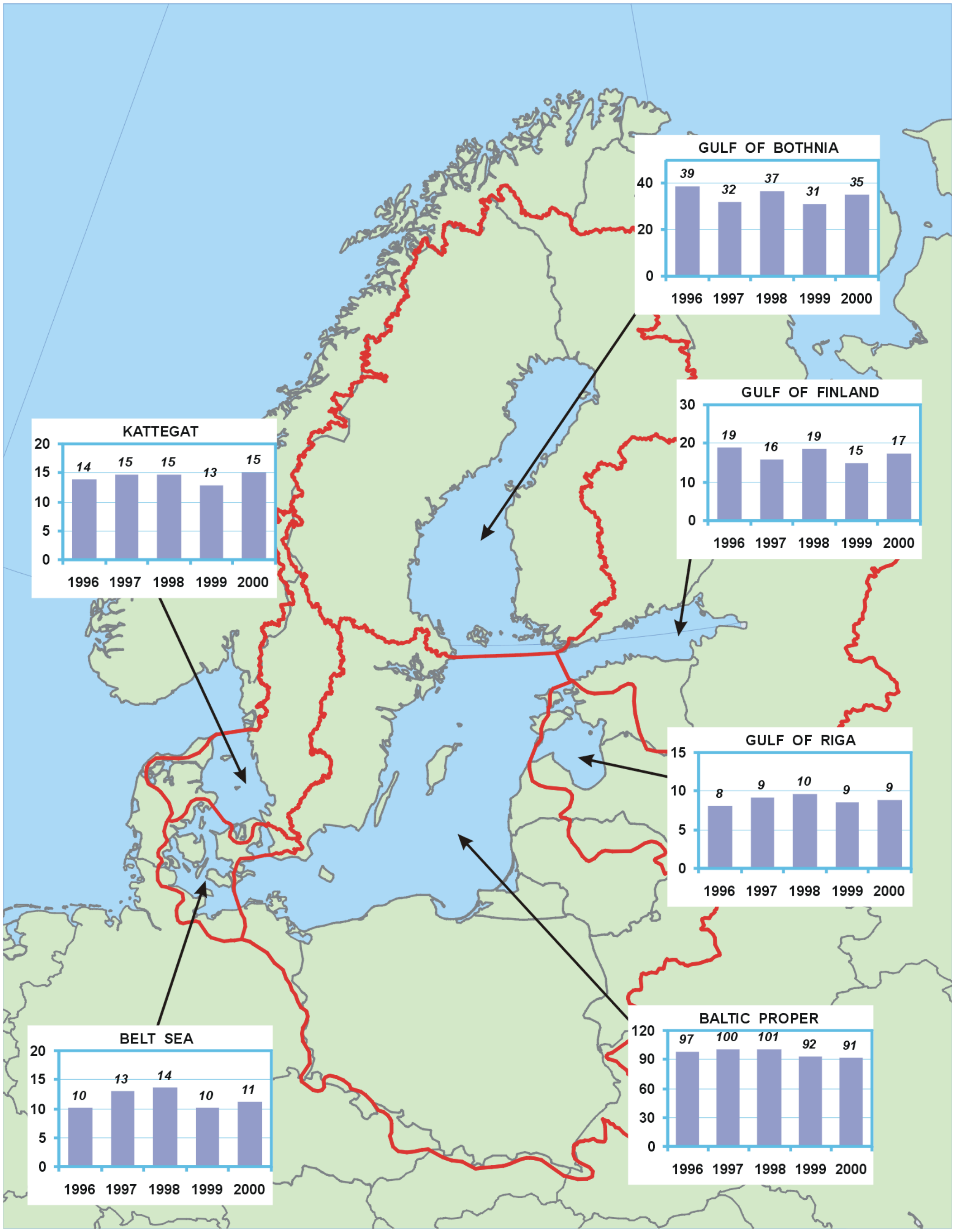

Figure 2.25. Time series of lead deposition to six main sub-basins of the Baltic Sea in the period 1996-2000. Units: tones/yr.

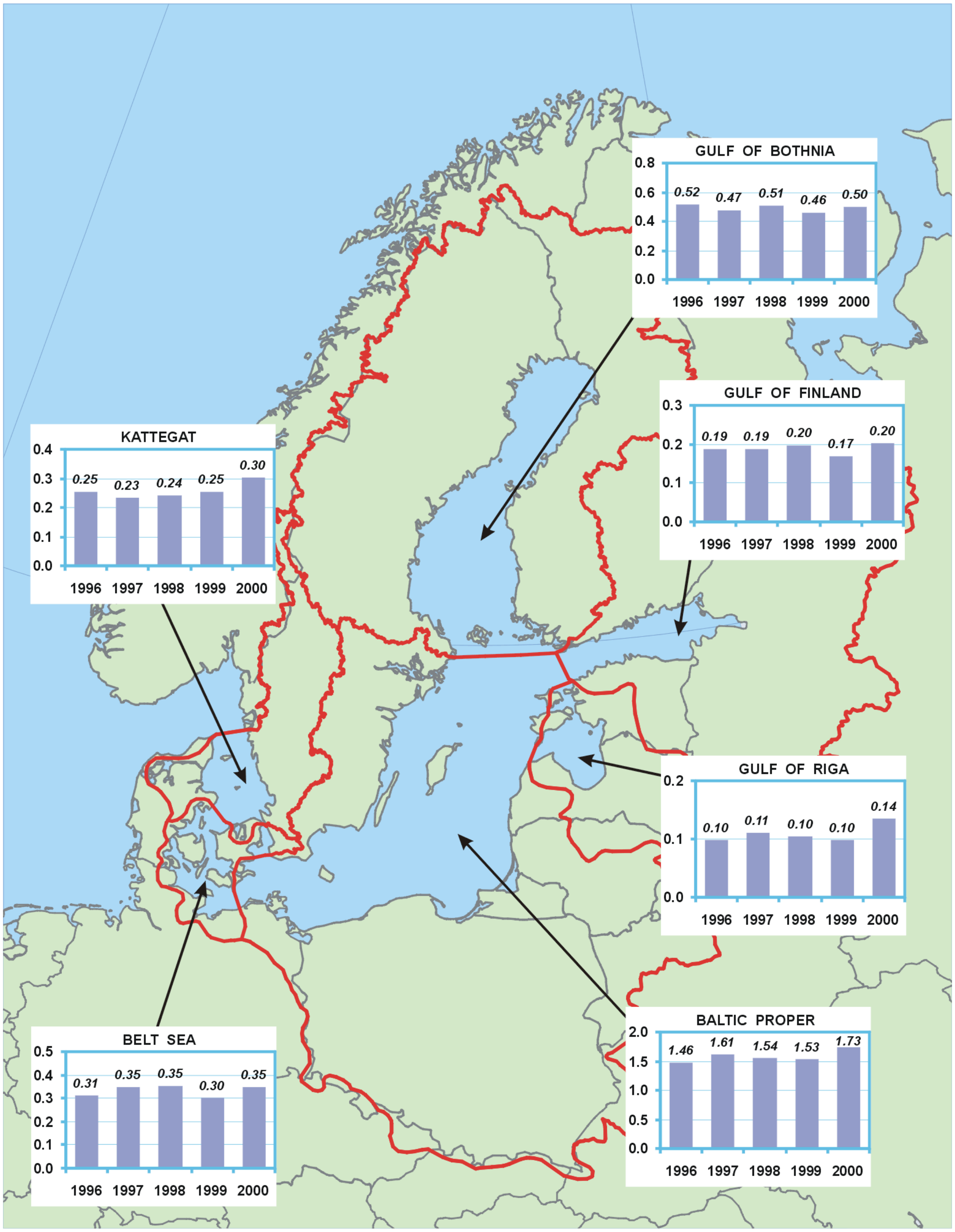

Figure 2.26. Time series of mercury deposition to six main sub-basins of the Baltic Sea in the period 1996-2000. Units: tones/yr.

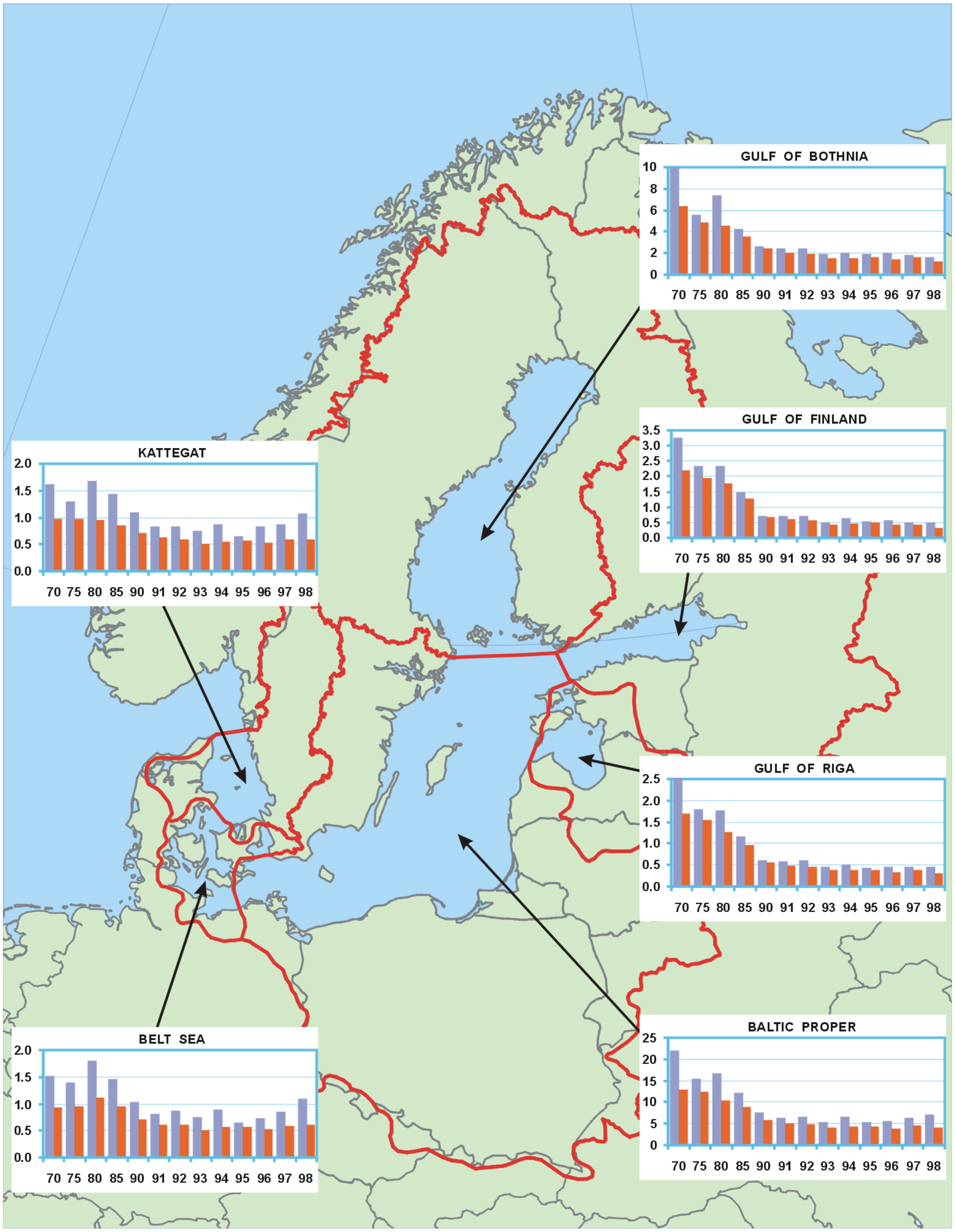

Figure 2.27. Time series of lindane deposition to and volatilization from the six sub-basins of the Baltic Sea for the period 1970-1998 in tonnes/yr.

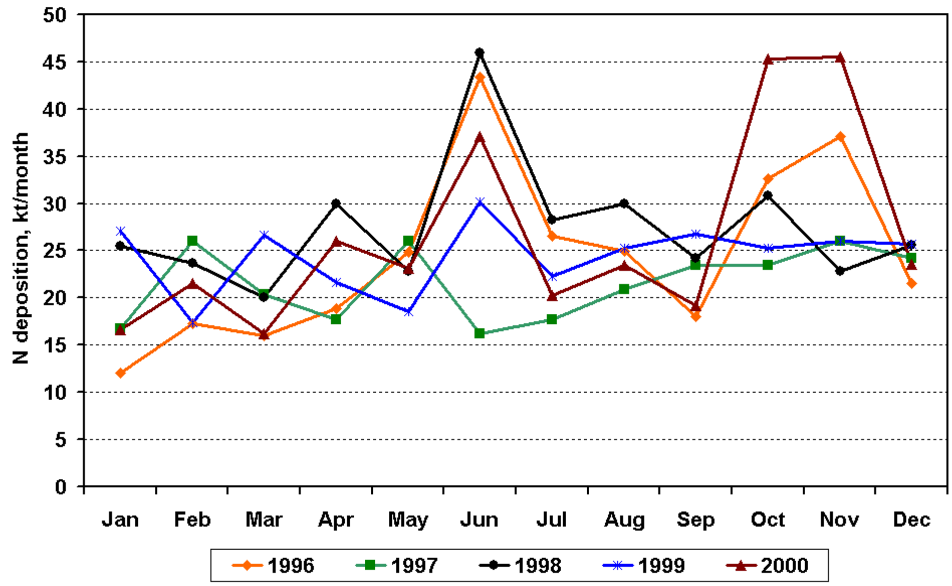

Figure 2.28. Seasonal variation of computed total nitrogen depositions to the Baltic Sea for the period 1996-2000 in ktonnes/month.

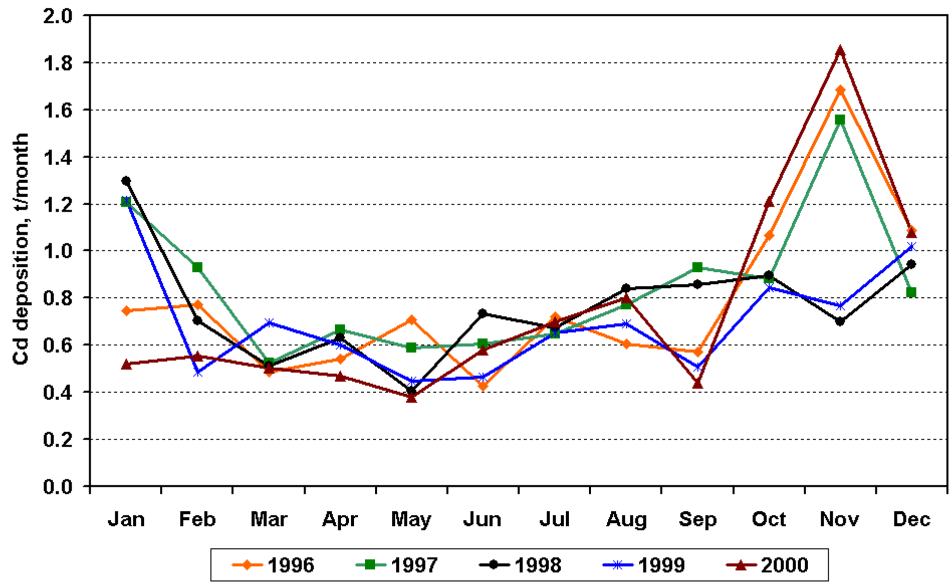

Figure 2.31. Seasonal variation of computed cadmium depositions to the Baltic Sea for the period 1996-2000 in tonnes/month.

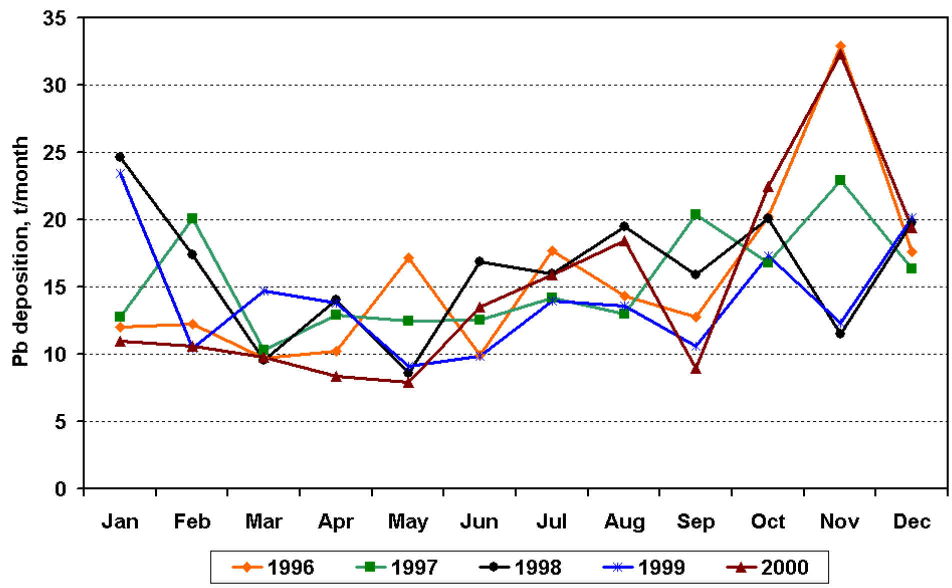

Figure 2.32. Seasonal variation of computed lead depositions to the Baltic Sea for the period 1996-2000 in tonnes/month.

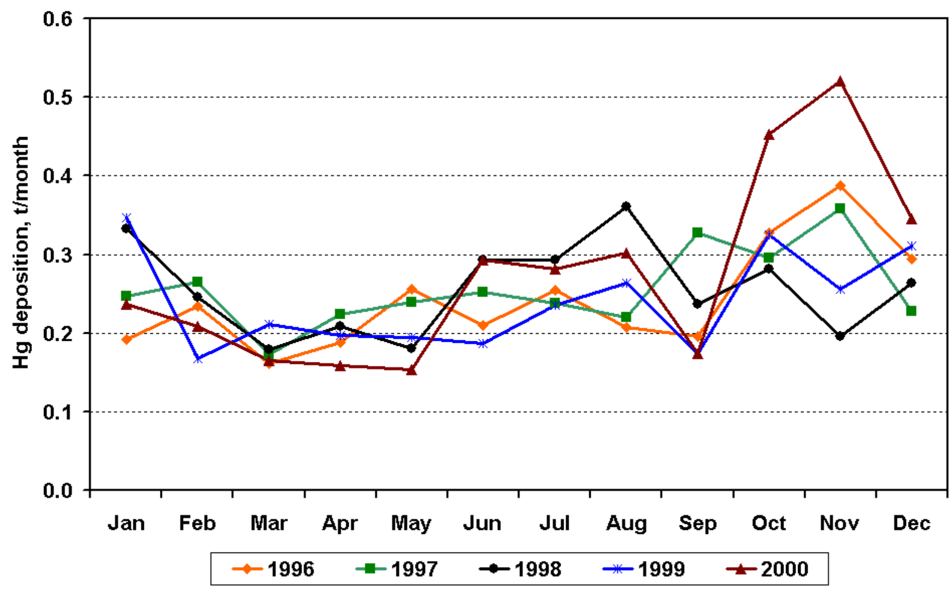

Figure 2.33. Seasonal variation of computed mercury depositions to the Baltic Sea for the period 1996-2000 in tonnes/month.

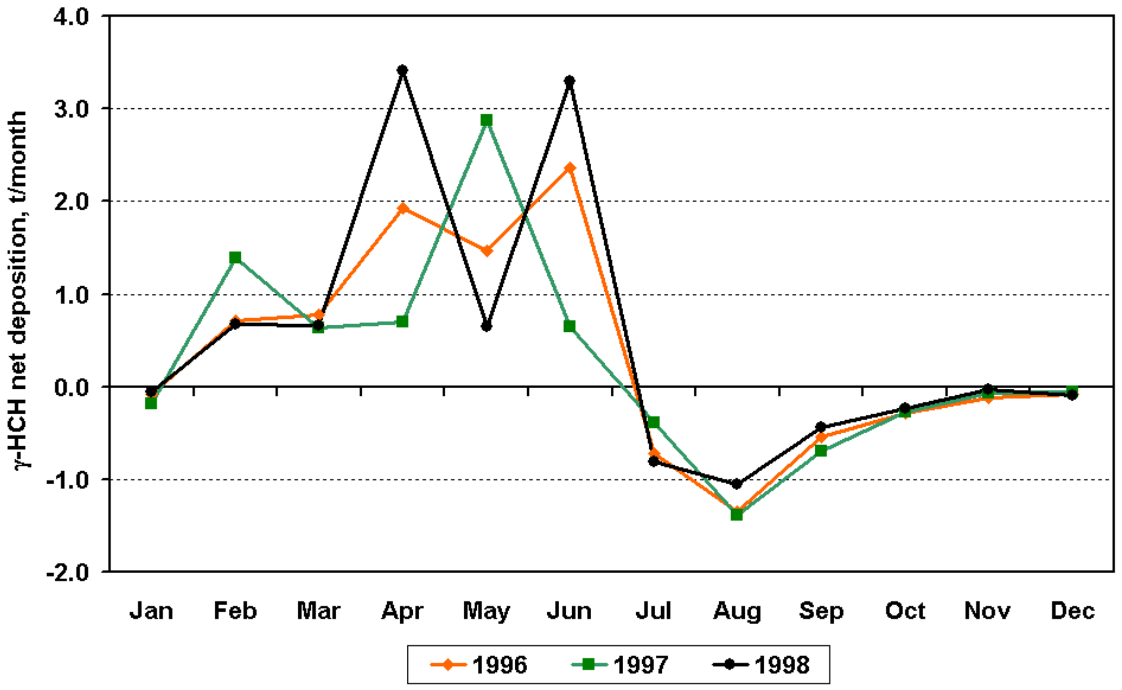

Figure 2.34. Seasonal variation of computed mercury depositions to the Baltic Sea for the period 1996-2000 in tonnes/month.